Int J Earth Sci (Geol Rundsch) (2006) 95: 34–49
DOI 10.1007/s00531-005-0020-3

ORIGINAL PAPER

Damien Dhont · Jean Chorowicz

Review of the neotectonics of the Eastern Turkish–Armenian Plateau by geomorphic analysis of digital elevation model imagery

Received: 21 June 2004 / Accepted: 18 June 2005 / Published online: 23 September 2005

Abstract Digital elevation model (DEM) images provide synoptic views of the Earth's surface allowing the analysis of landforms of still active tectonic and volcanic structures at regional scale. A DEM at 250 m pixel size constitutes regional scale data particularly efficient to investigate the late Miocene–Quaternary deformation of the Eastern Turkish–Armenian Plateau in the Arabian–Eurasian area of convergence. Geomorphic analysis of the DEM image associated with review of fault-plane solutions of earthquakes show that faults are mostly strike-slip with small vertical component. Here we show that the orientations of the tectonic and volcanic structures fit with a tectonic regime characterized by N–S shortening and E–W lengthening, consistent with westward escape of Anatolia perpendicular to the direction of the Arabia–Eurasia shortening. The uniform uplift of the plateau, the predominance of strike-slip faulting, the lack of major thrusts and the occurrence of normal faults do not support a model of going-on crustal thickening due to intracontinental convergence. On the contrary, our observations can be better interpreted in terms of lithospheric thinning and mantle upwelling related to gravity escape of Anatolia.

Keywords Anatolia · Neotectonics · DEM · Uplift · Escape tectonics

D. Dhont (✉)
FRE 2639: Imagerie Géophysique, CURS-IPRA, Université de Pau et des Pays de l'Adour, Avenue de l'Université, 64013 Pau cedex, France
E-mail: damien.dhont@univ-pau.fr
Tel.: +33-5-59407425
Fax: +33-5-59407415

J. Chorowicz
UMR 7072: Laboratoire de Tectonique, case 129, Université Pierre et Marie Curie, 4 place Jussieu, 75252 Paris cedex 05, France
E-mail: choro@lgs.jussieu.fr
Tel.: +33-1-44275089
Fax: +33-1-44275085

Introduction

The Eastern Turkish–Armenian Plateau (ETAP) forms a broad surface at 2,000 m mean elevation that is generally considered to be uplifting (Fig. 1). It is characterized by morphotectonic structures recognized in the field mostly during the 1960s–1970 s (Ambraseys and Zatopek 1968; Wallace 1968; Arpat and Saroglu 1972; Seymen and Aydin 1972; Tchalenko 1977; Toksöz et al. 1977). These preliminary observations have served as the basis for interpretations and discussions concerning the morphological, structural and volcanic evolution of the area (e.g., Saroglu and Güner 1981; Saroglu and Yilmaz 1986; Yilmaz et al. 1987; Sengör et al. 1985; Dewey et al. 1986; Adiyaman et al. 1998; Koçyigit et al. 2001). More recently, original geophysical data on the lithospheric structure of the ETAP have been published from a global seismic survey (Al-Lazki et al. 2003; Gök et al. 2003; Sanvol et al. 2003; Örgülü e al. 2003; Turkelli et al. 2003; Zor et al. 2003). The ages of the neotectonic and volcanic structures and uplift of the ETAP are coeval with the collision between the Arabian and Eurasian plates dated as middle-late Miocene (Sengör et al. 1985; Saroglu and Yilmaz 1986). In Eastern Turkey, the collisional area corresponds to the Bitlis belt, affected by thrusts verging south or north, and folds. To the north, the ETAP has been described to be dominated by compression, implying uplift, (Sengör and Kidd 1979; Saroglu and Yilmaz 1986) or by a strike-slip regime of deformation (e.g., Barka and Kadinsky-Cade 1988; Jackson 1992; McClusky et al. 2000; Koçyigit et al. 2001). Conversely, Gülen (1984) has described extension associated to strike-slip tectonics. The respective parts of compressional, strike-slip and extensional deformations being not well established, new structural and geomorphic analyses of the ETAP are critical for the understanding of the neotectonics of the plateau.

Topographic images derived from digital elevation models (DEMs) provide synoptic views of the earth surface, allowing the analysis of landforms of still active

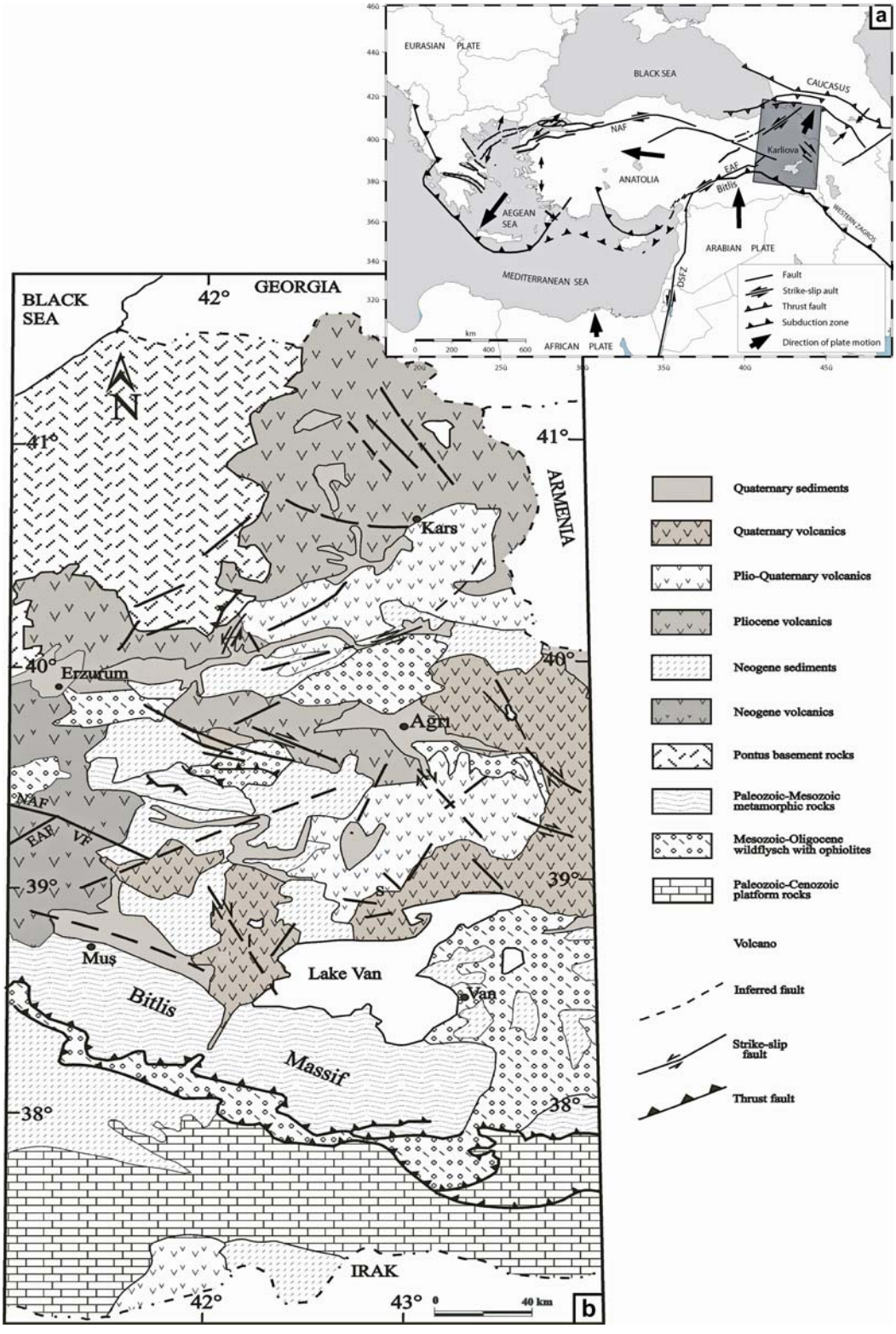

Fig. 1 Geological context of the Eastern Turkish–Armenian Plateau. **a** Geodynamic framework. *Rectangle* shows the study area. **b** Simplified geological map of the studied area, from the 1:2,000,000 geological map of Turkey (MTA 1989). *EAF* East Anatolian Fault; *NAF* North Anatolian Fault; *VF* Varto fault

tectonic and volcanic structures at regional scale (Dhont et al. 1998a, b; Kühni and Pfiffner 2001; Oguchi et al. 2003; Silva et al. 2003). Large-scale structures are well observed from a DEM with resolution of 250 m pixel-size. The aim of this paper is to show that the DEM constitutes first-order valuable data for detailed geo-

morphic analysis at regional scale, helping to implement the mapping of the main neotectonic structures of the ETAP. We shall describe patterns showing the prevalence of strike-slip extensional (transtensional) tectonics in the area.

Overview of the study area

The ETAP is located between two collisional areas, the Bitlis–Zagros belt to the south and the Caucasus mountains to the north (Fig. 1a). The neotectonic context of the area is in keeping with the general geodynamic pattern of the Eastern Mediterranean [see Bozkürt (2001) for a review]. North-south intracontinental collision between Arabia and Eurasia since the middle-late Miocene (Sengör and Yilmaz 1981; Sengör et al. 1985) and initiation of back-arc extension in the Aegean Sea since the late Oligocene (Jolivet et al. 1994; Jolivet and Patriat 1999) are the boundary conditions allowing the westward mass transfer of Anatolia, frequently considered as a rigid plate bounded by the North Anatolian Fault (NAF) and the East Anatolian Fault (EAF) meeting at Karliova. Anatolian westward motion has been considered to have initiated in the early Pliocene (Dhont et al. 1998a; Koçyigit and Beyhan 1998; Platzman et al. 1998; Armijo et al. 1999; Barka et al. 2000). Chorowicz et al. (1999) proposed that the NAF propagated eastward beyond Karliova as far as the Varto fault, which runs across the ETAP (Fig. 1b). This plateau is half-covered with volcanic rocks (e.g., Innocenti et al. 1982; Yilmaz et al. 1987, 1998), whose ages range from 11 Ma (late Miocene) to the Quaternary (Keskin et al. 1998). Several neotectonic structures of different orientations cross-cut the ETAP: NE-striking left-lateral strike-slip faults, NW-striking right-lateral strike-slip faults, E-striking reverse faults, and N-striking normal faults and/or fissures that gave rise to volcanic activity (Saroglu and Güner 1981; Koçyigit 1985; Sengör et al. 1985; Dewey et al. 1986; Barka and Kadinsky-Cade 1988; Koçyigit et al. 2001).

GPS data show that the Arabia–Eurasia compressive strain is predominantly distributed into strike-slip deformations in the ETAP and crustal shortening occurring mainly in the Caucasus (Reilinger et al. 1997; McClusky et al. 2000), with no or little underthrusting of the Arabian plate under Eurasia along the Bitlis belt (Al-Lazki et al. 2003 ; Turkelli et al. 2003; Zor et al. 2003). From the analysis of satellite and low-resolution DEM images of part of this area, Adiyaman et al. (1998) mapped the faults that are only related with volcanoes. In agreement with Gülen (1984), they concluded that strike-slip motion is often associated with vertical throws.

Approach

Our main aim is to use DEM imagery in order to implement the knowledge of the largest neotectonic structures in the ETAP. The shadowed and hypsometric colored DEM image (Fig. 2a) was generated by interpolation at 250 m ground pixel of digitized contours from topographic charts at scale 1:250,000. This DEM constitutes the basis for geomorphic analysis at regional scale. The faults we have mapped can be considered as the main ones because they are clearly displayed on such an image.

Neotectonic faults can be identified by (1) their morphology, forming asymetric ranges with one side corresponding to breaks in slope or scarps, (2) the displacement of late Neogene volcanic boundaries, structural or erosional surfaces, and (3) the occurrence of straight lines of several tens of kilometers in length. We have systematically compared our images with geological maps in order to carefully separate the scarps formed by fault planes (active) from those resulting from differential erosion of contrasted lithology (ancient). The active fault scarps, even eroded, are much higher and longer than the scarps formed by lithological contrasts.

We have identified when possible the strike-slip, normal or reverse nature of the faults. Strike-slip faults have rectilinear traces and they locally bound push-up hills or extensional basins at step-over or bends of the fault trace. They can be associated with typical patterns such as tail-crack or horse-tail structures at fault ends. Reverse faults have sinuous traces and they are associated with half-cylindrical-shaped hills of the uplifted blocks due to drag folds deforming ancient planar erosion surface in the hanging wall. Normal faults are recognized by the following geomorphic characters: (1) they generally have a widely arched trace, concave (mainly) or convex toward the footwall, in contrast to the strike-slip faults whose trace is generally straighter; (2) they bound tilted plateaus (tilted blocks); (3) as is also the case for the strike-slip faults, they are not related to half-cylindrical-shaped hills corresponding to recent drag folds, which accompany active reverse faulting. We have also mapped the recent folds, the synclines, forming lowlands filled with sediments, and the anticlines corresponding to regularly shaped elongate hills. It is important to point out that this approach provides information on the finite strain, but not on its detailed history. Our observations take into account finite deformation from the late Miocene to the Present.

The ETAP is covered by a number of volcanoes that also can be indicators of the tectonic strain regime (e.g., Nakamura 1977). The emplacement of volcanoes can be related to local scale tectonic structures such as tension fractures (Opheim and Gudmundsson 1989; Chorowicz et al. 1997; Korme et al. 1997; Dhont et al. 1998b) or open faults (Cello et al. 1985; Chorowicz et al. 2001). We have mapped the volcanic edifices forming a pattern of elongate volcanoes or linear clusters of adjacent volcanoes. Once we have inferred the geometry of these vents, we have used them as ordinary vertical open fractures to deduce the local strain from their orientation.

In order to implement these structural data, we have also plotted on the DEM (Fig. 2b) the fault-plane

solutions of major earthquakes ($Ms > 4$) that occurred in the area (Table 1).

Geomorphic analysis of the DEM

Geomorphic analysis at local scale

Faults

Faults with major reverse component In the south, the DEM image (Fig. 2) displays the Bitlis belt, bounded by the northern and southern Bitlis thrust faults. Compression is attested by the fault-plane solutions 6 and 24. Within the Bitlis massif, a N70°E- and N120°E-trending continuous segment is clearly visible, respectively west and east of long. 41°E. This line separates the north-verging and south-verging thrust fronts and forms the structural axis of the Bitlis belt. It would represent the surface expression of the Bitlis suture in depth (Dhont 1999).

The Mus and Lake Van basins lie immediately to the north of the Bitlis belt. They have been regarded as ramp basins of compressional origin on the basis of interpretations of seismic sounding, earthquake focal mechanisms (fault-plane solution 17), photographs, and satellite images (McKenzie 1972; Sengör and Kidd 1979; Sengör et al. 1985). Conversely, Dewey et al. (1986) noticed that Quaternary volcanic deposits around Lake Van remain unfolded. Gülen (1984), re-interpreting seismic profiles of Wong and Finckh (1978), concluded that there are no major thrusts in these basins but mainly oblique-slip normal faults associated with subsidence. The DEM shows that the Mus basin is bounded to the north by the Otluk fault, which does not have the morphology of a reverse fault. Its trace is not sinuous but slightly curved. It forms the southern boundary of a tilted block represented by a planar erosion surface dipping to the north. The Nemrut volcano is located at the eastern termination of the fault in a tail crack position, showing that the Otluk fault has a dextral strike-slip component. We then interpret the Mus basin as an oblique-slip half-ramp basin bounded to the south by the northern Bitlis thrust and to the north by the transtensional dextral oblique-slip Otluk fault (Fig. 2b).

To the north, the Pasinler and Erzurum basins appear to be structures similar to each other. Their southern and northern ~N60°E-trending margins are bounded by fold-shaped hills accompanying sinuous fault traces, which we interpret as thrust ramps (Fig. 2b). South of the Pasinler basin, the 07 November 1985 earthquake indicates that thrusting is associated with strike-slip movement (fault-plane solution 14 on Fig. 2b). Both the Pasinler and Erzurum basins end to the east in left-lateral transcurrent faults striking respectively NNE-SSW (Erzurum fault; Barka and Kadinsky-Cade 1988) and NE-SW (Cobandede fault; Koçyigit et al. 2001). These basins have been interpreted as pull-apart structures opening in relay zones located at left-stepping offset of the N60°E-trending left-lateral faults bounding the northern and southern margins of the basins (Atalay 1978; Koçyigit et al. 2001). In our opinion they cannot be pull-apart basins because they do not have a distinct rhomb-shaped geometry, and their northern and southern faulted margins have a noticeable reverse component. These basins can be better interpreted as oblique-slip ramp basins, as it was previously suggested by Sengör et al. (1985).

Cutting through the northern part of the region, the Pambak-Sevan fault zone (PSFZ in Fig. 2b) is a large-curved fault zone that progressively changes from E-W to NE-SW strike respectively north and west of Kars, where to the west it continues as the left-lateral strike-slip Cobandede fault. The PSFZ may have the morphology of a reverse fault bounded to the north by narrow continuous fold-shaped hills rather than by a normal fault, but fieldwork will be necessary to determine the slip motion. It connects eastward with a major structure corresponding to the Lesser Caucasus suture zone (Rebaï et al. 1993; Koçiyit et al. 2001). More to the north, the Spitak event (plot 18) is one of the major earthquakes of this area. The fault scarp related to this event is visible on the DEM and the fault-plane solution together with field observations (e.g., Bommer and Ambraseys 1989; Cisternas et al. 1989) indicate thrusting with a small strike-slip component.

The N30°E-trending Olur fault lies 75 km northwest of the PSFZ. It is bounded on its west side by an elongate uplifted convex surface. The surface lies above the Ardahan basin to the east, which has been interpreted as a pull-apart basin (Koçyigit et al. 2001). However, this basin does not have a rhomb-shaped geometry and moreover it does not correspond to a fault step. We interpret that the crest line of the elongate hill corresponds to the hinge of a N20°E-trending anticline forming a drag fold associated with the thrust motion along the Olur fault. In this context, the Ardahan basin is interpreted to be a syncline drag fold formed in the footwall of the fault.

Strike-slip faults Strike-slip faults constitute the main neotectonic structures of the ETAP. Most of them have been described in the literature (e.g., Yilmaz et al. 1987; Saroglu et al. 1992; Sengör et al. 1985; Koçyigit et al. 2001) and have a clear expression on the DEM. This is the case for the Kelkit-Coruh, Erzurum, Narman, Senkaya-Göle, Cobandede, Horasan, Kagizman, Karaçoban, Süphan and East Anatolian left-lateral strike-slip faults, and the Agri, Hamur, Balik Gölü and North Anatolian right-lateral strike-slip faults (Fig. 2b).

The Erzurum, Narman and Sengaya-Göle fault zones (near long. 42°E, lat. 40°30'N) consist of several NE-trending fault segments bounding elongate hills corresponding to recently uplifted erosion surfaces. We interpret these domes as restraining bend structures that formed at right-stepping relays of the fault system. Focal

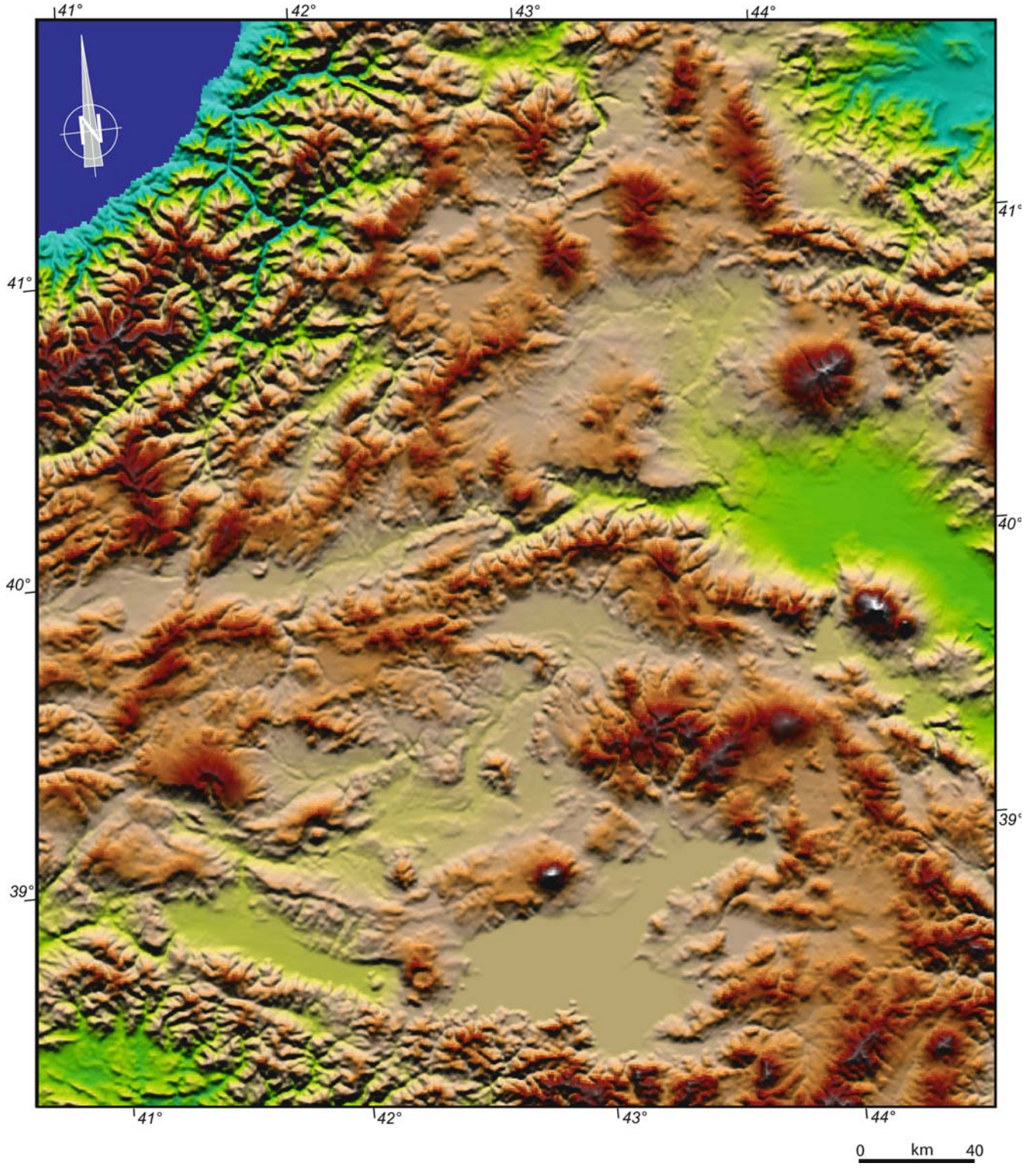

Fig. 2 **a** Shadowed image of a digital elevation model (DEM) of the Eastern Turkish–Armenian Plateau. It has been generated by linear interpolation of digitized elevation contour lines of the 1:250,000 scale topographic chart of Turkey. Pixel size is 250 m. Illumination is from the north. **b** Structural analysis of the DEM. *AF* Agri fault; BGF Balik Gölü fault; *BFZ* Baskale fault zone; *CF* Caldiran fault; *CbF* Cobandede fault; *DF* Diyadin fault; *EAF* East Anatolian Fault; *EF* Erzurum fault; *HGF* Hasantimur Gölü fault; *HaF* Hamur fault; *HoF* Horasan fault; *HiF* Hinis fault; *KçF* Karaçoban fault; *KCFZ* Kelkit-Coruh fault zone; *KgF* Kagizman fault; *KyF* Karayazi fault; *LCSZ* Lesser Caucasus suture zone; *MF* Malazgirt fault; *NAF* North Anatolian Fault; *NFZ* Narman fault zone; *OlF* Olur fault; *OtF* Otluk fault; *PSFZ* Pambak-Sevan fault zone; *SGF* Sengaya-Göle fault; *SF* Süphan fault; *TF* Tutak fault; *TLF* Tuzluca fault; *VF* Varto fault. *AkV* Akca Volcano; *AbV* Akbaba volcano; *AV* Akdogan volcano; *BiV* Bingöl volcano; *BV* Bilican volcano; *CaV* Cavahet volcano; *CV* Ciplak volcano; *GV* Girekol volcano; *HV* Hayal volcano; *KV* Kandil volcano; *KaV* Kavak volcano; *KeV* Kel volcano; *KiV* Kisir volcanoes; *LeV* Legli volcano; *MV* Meydan volcano; *NV* Nemrut volcano; *SV* Süphan volcano; *SbV* Sübhan volcano; *TV* Tendurek volcano; *YV* Yillik volcano; *ZtV* Ziarettepe volcano; *ZV* Zor volcano

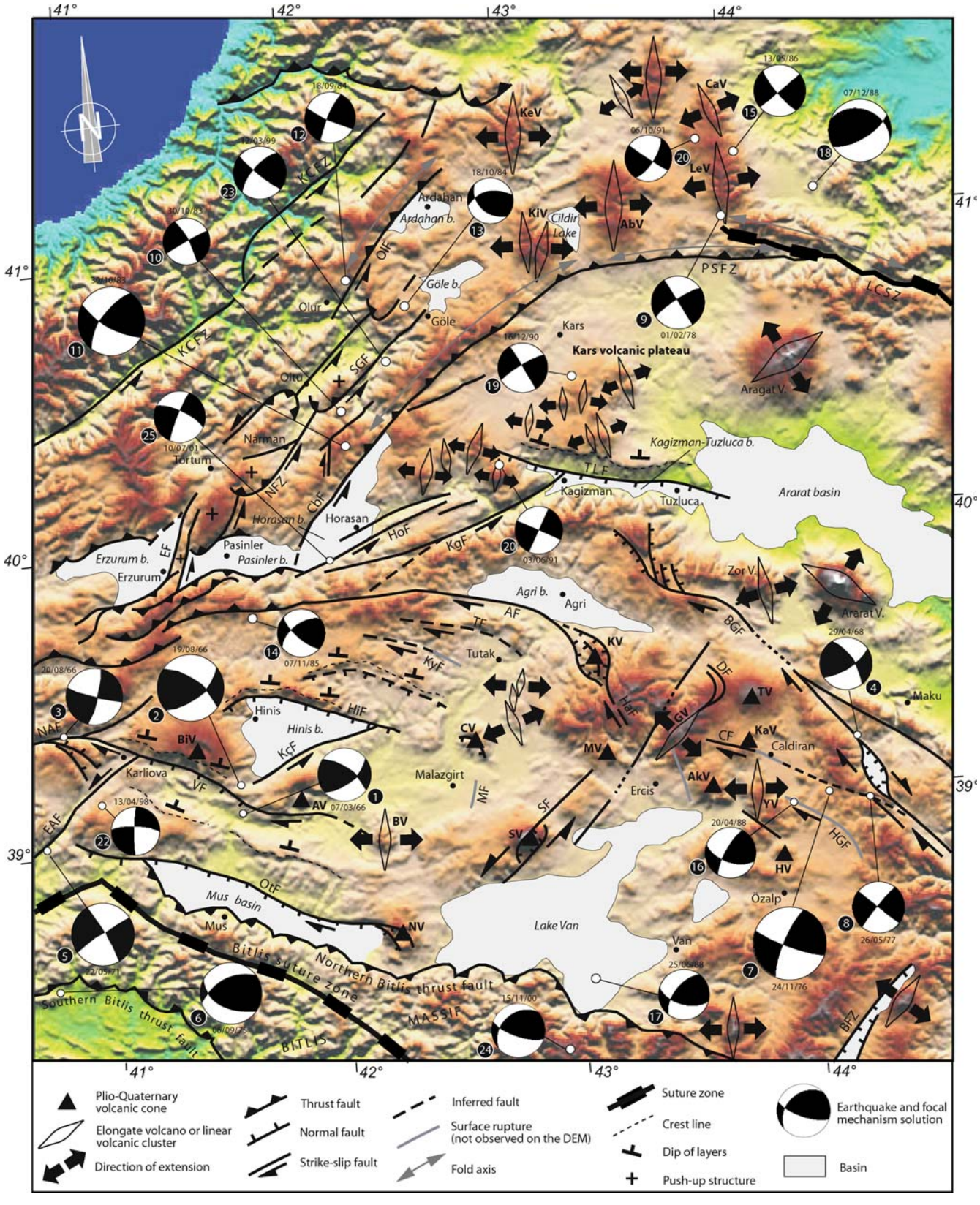
41°
42°
43°
44°
41°
40°
39°
N
18/09/64
12/03/99
30/10/83
30/10/83
10/07/91
19/08/66
20/08/66
07/11/85
07/03/66
13/04/98
22/05/71
06/09/75
18/10/84
06/10/91
13/05/86
07/12/88
16/12/90
01/02/78
03/06/91
29/04/68
20/04/88
25/05/88
24/11/76
26/05/77
15/11/00
KCFZ
OlF
SGF
NFZ
CbF
HoF
KgF
EF
AF
TF
KyF
HlF
KcF
VF
EAF
NAF
OtF
MF
SF
HaF
DF
CF
HGF
TLF
PSFZ
LCSZ
BGF
BFZ
KeV
KiV
AbV
CaV
LeV
BiV
AV
BV
CV
MV
NV
SV
KV
TV
GV
KaV
AkV
YV
HV
Ardahan
Ardahan b.
Cildir Lake
Göle b.
Olur
Göle
Kars
Kars volcanic plateau
Aragat V.
Oltu
Narman
Tortum
Horasan b.
Horasan
Kagizman-Tuzluca b.
Kagizman
Tuzluca
Ararat basin
Pasinler
Pasinler b.
Erzurum b.
Erzurum
Agri b.
Agri
Zor V.
Ararat V.
Maku
Tutak
Hinis
Hinis b.
Karliova
Malazgirt
Ercis
Caldiran
Özalp
Van
Lake Van
Mus
Mus basin
Bitlis suture zone
Northern Bitlis thrust fault
Southern Bitlis thrust fault
MASSIF
BITLIS
Plio-Quaternary volcanic cone
Elongate volcano or linear volcanic cluster
Direction of extension
Thrust fault
Normal fault
Strike-slip fault
Inferred fault
Surface rupture (not observed on the DEM)
Fold axis
Suture zone
Crest line
Dip of layers
Push-up structure
Earthquake and focal mechanism solution
Basin

Fig. 2 (Contd.)

Table 1 Parameters of focal mechanism solutions for earthquakes in the Eastern Turkish–Armenian Plateau. Senses of motion along the observed fault plane are L (*left-lateral*), N (*normal*), R (*right-lateral*) and T (*thrust*), and any of these combinations (compilation of Ambraseys and Jackson 1998)

Reference number on Fig. 2b	Fault plane solution reference	Date (d/m/y)	Epicentre		Magnitude (Ms)	Field observations		
			Lat. (N°)	Long (E°)		Sense of motion	Horizontal displacement (cm)	Vertical displacement (cm)
1	(c)	07/03/1966	39.10	41.40	6.2 (d)	RN	5	20
2	(c)	19/08/1966	39.20	41.60	6.9 (a)	RN	30	25
3	(c)	20/08/1966	39.30	41.16	6.3 (f)			
4	(c)	29/04/1968	39.20	44.30				
5	(a)	22/05/1971	38.90	40.64	6.8 (f)	L	38	60
6	(a)	06/09/1975	38.55	40.75	6.5 (f)	T	–	60
7	(b)	24/11/1976	39.10	44.00	7.26 (f)	R	350	50
8	(b)	26/05/1977	38.70	44.32	5.4 (a)			
9	(b)	01/02/1978	41.23	44.03	5.1 (b)			
10	(e)	30/10/1983	40.45	42.17	5.1 (e)			
11	(e)	30/10/1983	40.28	42.18	6.8 (e)	L	100	60
12	(e)	18/09/1984	40.90	42.24	5.5 (e)			
13	(e)	18/10/1984	40.79	42.48	5.1 (e)			
14	(b)	07/11/1985	39.75	41.68	4.2 (b)			
15	(b)	13/05/1986	41.03	43.92	5.4 (b)			
16	(b)	20/04/1988	38.97	44.00				
17	(b)	25/06/1988	38.44	43.08	5.0 (b)			
18	(b)	07/12/1988	40.85	44.13	6.76 (f)	RT	150	50
19	(b)	16/12/1990	40.53	43.18	5.0 (b)			
20	(b)	03/06/1991	40.22	42.82	4.1 (b)			
21	(b)	06/10/1991	41.29	43.85	4.4 (b)			
22	(b)	13/04/1998	39.18	41.10	4.8 (b)			
23	(b)	12/03/1999	40.61	42.40	5.5 (b)			
24	(b)	15/11/2000	38.30	42.92				
25	(b)	10/07/2001	39.94	42.07				

(a) Jackson and McKenzie, 1984
(b) Harvard cmt
(c) McKenzie, 1972
(d) Ambraseys and Jackson, 1998
(e) Eyidogan et al. 1999
(f) Ambraseys, 2001

mechanisms indicate compression (fault plane solution 13) but this is local and the motion is predominantly left-lateral strike-slip with a small thrust component (plots 10, 11, 12, and 23) in agreement with our interpretation.

The emplacement of the volcanic vents can be related to faults, especially in extensional relay zones. This is the case for the Süphan volcano (long. 42°50′, lat. 38°50′) which is rooted in a transtensional zone that opened in a left-stepping offset of the Süphan fault. The Kandil volcano (long. 43°20'E, lat. 39°35'N) is another volcanic vent related to a tensional structure. It is located at the curvature between the E-trending Agri and NW-trending Hamur right-lateral faults, and probably occupies a releasing bend opening.

South of the Ararat basin, the N120°E-trending Balik Gölü fault has a clear right-lateral displacement evidenced by a pull-apart basin and a horse-tail pattern at the fault termination. Right-lateral strike-slip motion can be locally associated with a minor reverse component as attested by the fault-plane solution of the 29 April 1968 earthquake (plot 4).

Other faults are not well shown in detail by the DEM image and we did not find morphological evidence to give their sense of motion. However, fault-plane solutions and published field observations have been made along active faults. Focal mechanisms of earthquakes associated with the Caldiran fault (plots 7 and 8) indicate dextral strike-slip movement, consistent with the field observations of Arpat et al. (1977). The Hasantimur Gölü fault is right-lateral strike-slip with a reverse component (plot 16). Field structural observations indicate right-lateral strike-slip movement along the Tutak (Saroglu and Güner 1979) and Karayazi (Kocyigit 1985; Koçyigit et al. 2001) faults (long. 43°E, lat. 39°40′N).

In the northeastern corner of the image, fault traces are not well displayed on the DEM image, but several earthquakes have occurred (plots 9, 15 and 20) whose focal mechanisms are predominantly strike-slip and associated with small normal throws (plots 15 and 20). We could not identify fault scarps in the Kars volcanic area although earthquakes occurred and indicate strike-slip deformation (plot 19).

The eastern terminations of the NAF and EAF are displayed in the western part of the DEM image. Fault-plane solutions associated with earthquakes indicate respectively right-lateral (plot 3) and left-lateral (plot 5) strike-slip motion, both of them containing a minor normal component along the principal nodal plane. The NAF continues to the east beyond Karliova forming the Varto fault. The fault scarp, well displayed on the image, bounds a depressed surface in the south and cuts the

Bingöl volcano. Prolongation of the NAF farther east, well beyond the Karliova triple junction, is also imaged by a continuous band of seismicity (Turkelli et al. 2003). Fault-plane solution along the Varto fault indicates right-lateral transpression (plots 1 and 2), whereas field observations (Wallace 1968; Ambraseys and Zatopek 1968) indicate extension, in agreement with the structural mapping of Chorowicz et al. (1999). A few kilometers east of the EAF, a fault-plane solution accounts for strike-slip deformation with a small normal component (plot 22).

Faults with a major normal component The Hinis fault, situated north of the Varto fault, is a S-dipping normal fault separating the Hinis basin from a tilted block. Immediately to the north, the DEM image displays a similar structure that is more eroded. These faults have large-curved traces in plan view, showing that they probably root at shallow level in the crust.

South of the Kars volcanic plateau, the DEM image displays the quite rectilinear N110°E-trending Tuzluca fault scarp that juxtaposes an uplifted flat erosion surface dipping northward to the north, and the narrow and elongate Kagizman-Tuzluca basin to the south. Koçyigit et al. (2001) interpreted this basin as a pull-apart structure. However it does not have a rhomb-shaped geometry and there are no dog-leg relays along the Tuzluca fault that would allow the opening of such a transtensional basin. The Tuzluca fault can be best viewed as a south-dipping normal fault bounding the Kagizman–Tuzluca basin in the hanging wall.

Open fractures

Extensional fractures and fissures localize elongate volcanic edifices or craters and clusters of aligned vents in the ETAP (Sengör and Kidd 1979; Sengör et al. 1985; Dewey et al. 1986; Adiyaman et al. 1998; Yilmaz et al. 1998). Open fractures were described at the summits of isolated Plio-Quaternary volcanoes such as the Nemrut, Tendurek, and Ararat edifices (Koçyigit et al. 2001).

North of the Kars Plateau, several tension fractures can be deduced from volcanoes. They strike mostly north (from N160°E to N10°E) and correspond to a minimum stress component $\sigma 3$ varying from N70°E to N100°E. Other elongate volcanoes indicate a $\sigma 3$ component varying from N30°E (Ararat volcano) to N160°E (Aragat volcano). In the southeastern corner of the image, a N20°E-trending open fracture is parallel to the Baskale fault zone forming an elongate graben.

Geomorphic analysis at regional scale

We have produced a DEM at ~2,000 m horizontal resolution by computation from the GTOPO30 data set using contours at 1,000 ft (~305 m) interval. Then we have applied several filters in order to emphasize the major geomorphic structures (ranges, deep basins, low plains) of the area (Fig. 3). The initial DEM was smoothed using a fast Fourier transform Butterworth filter in order to mask the major volcanic edifices and to remove the drainage network. The smoothing was achieved by accounting for the 10% most important frequencies, considering long wavelengths in order to reconstruct the topography (Harrison and Lo 1996; Collet et al. 2000). From this DEM, we have made a series of N-S topographic cross-sections extending from the Greater Caucasus up to the Arabian foreland (Fig. 4). The main geomorphic units visible both on the DEM and on the cross-sections are, from north to south: the Greater and Lesser Caucasus, the Pontides belt, the ETAP, the Bitlis belt and the Arabian platform.

The Arabian platform is a flat-lying surface affected by fold reliefs when approaching the Arabia-Eurasia collisional front. Elevations of the Bitlis and Western Zagros belts are surprisingly low (1,700—2,200 m) when considering they began to uplift during middle Miocene time (e.g., Sengör and Yilmaz 1981). Cross-sections (Fig. 4) reveal that these belts have lower altitudes than the ETAP, indicating that the collisional zone uplifts less rapidly than the plateau. East of long. 42°E, the Western Zagros merges with the ETAP and the folds of the Arabian platform, making difficult to identify it (Fig. 3). The ETAP, lying at ~2,000 m mean elevation in its central part (Fig. 5), forms a near horizontal surface except at local places of basins and volcanoes (Fig. 3). It is juxtaposed to the Eastern Pontides, at higher elevation, along a curved tectonic lineament corresponding to an Eocene suture zone (e.g., Sengör et al. 1985), which was probably reactivated in the Neogene to form the left-lateral strike-slip North-East Anatolian Fault (Yilmaz et al. 2000). To the north, the Greater Caucasus constitutes the highest belt in the area, with peaks reaching more than 5,500 m.

Discussion and conclusions

Several authors have proposed that the ETAP has been subjected to compression since the middle Miocene (Sengör and Kidd 1979; Sengör and Yilmaz 1981; Sengör et al. 1985; Saroglu and Yilmaz 1986), or the early Miocene (Yilmaz et al. 1987). However, Pearce et al. (1990) observed that folding of the post middle Miocene strata north of the Bitlis belt is minor. These observations are consistent with recent fault plane solutions of small-to-moderate earthquakes (Örgülü et al. 2003), indicating that most of the Arabia–Eurasia collision is taken up by strike-slip faults. Gülen (1984) established that the deformation is dominated by a NW-SE and NE-SW-trending conjugate set of major strike-slip faults associated with extensional tilted blocks. Koçyigit et al. (2001) presented evidence for a strike-slip faulting-dominated compressional–extensional tectonic regime in the Plio-Quaternary, compression having occurred during the Oligo–Miocene. Our analysis of the

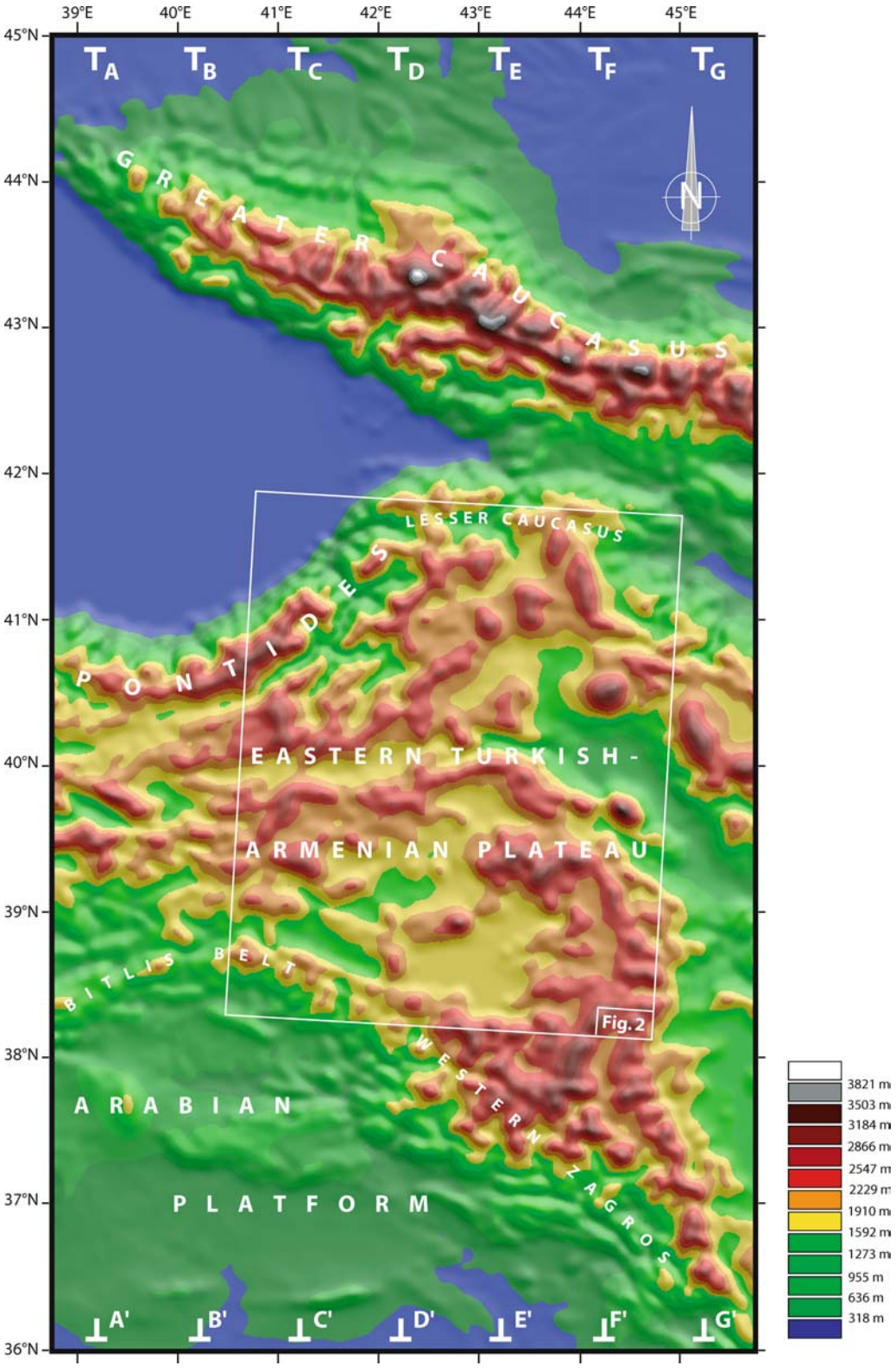

Fig. 3 Digital elevation model produced by smoothing an initial DEM at 2,000 m spatial resolution derived from the GTOPO30 database with a fast Fourier transform Butterworth filter that was achieved by accounting for the 10% most important frequencies. Letters refer to cross-sections of Fig. 4

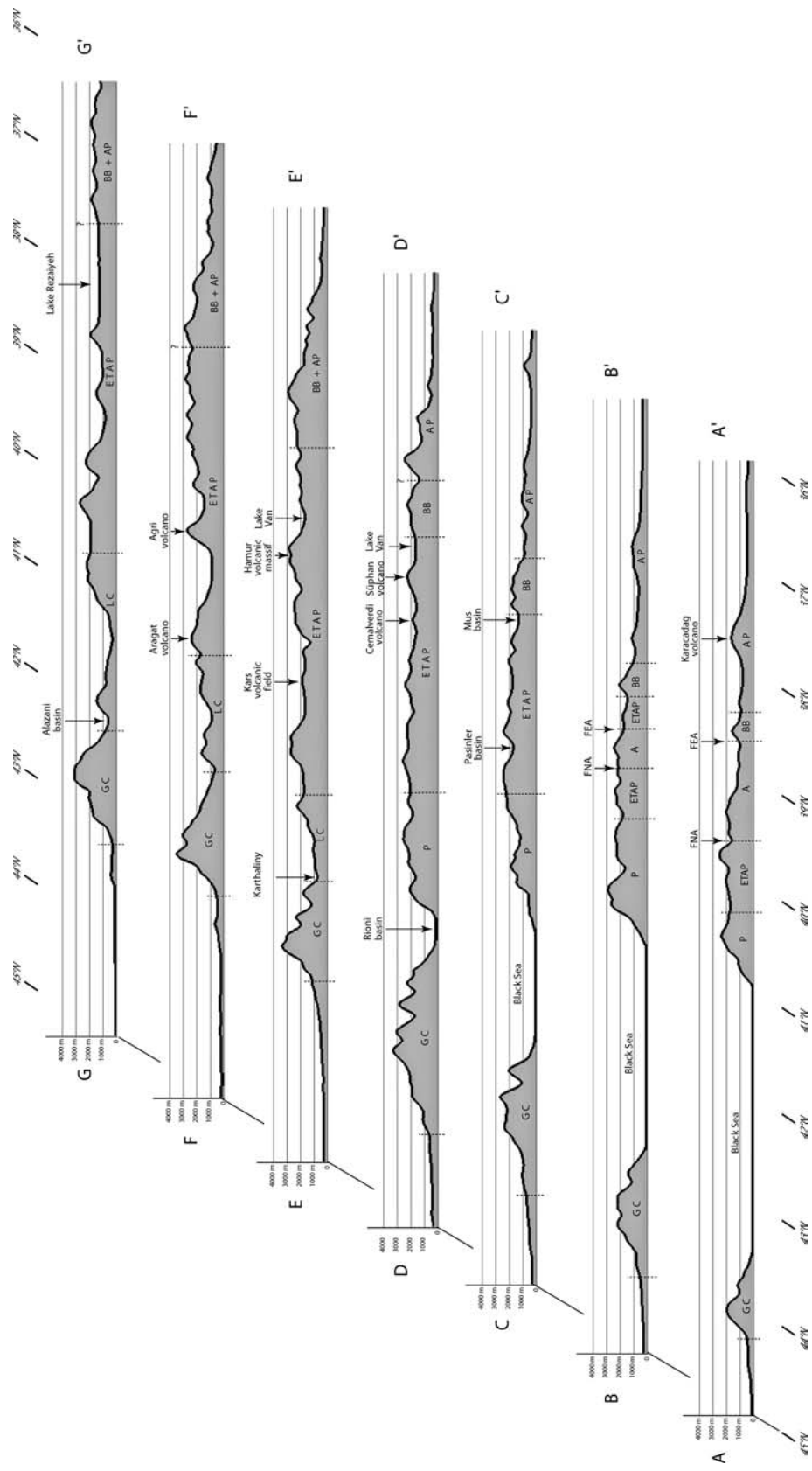

Fig. 4 Cross-sections derived from Fig. 3. *A* Anatolia; *AP* Arabian platform; *BB* Bitlis belt; *ETAP* Eastern Turkish-Armenian plateau; *GC* Greater Caucasus; *LC* Lesser Caucasus; *P* Pontides

DEM image, together with fault-plane solutions (Fig. 2), shows that the major faults are mostly strike-slip with small vertical components, either reverse or normal. This is consistent with the interpretations derived from slip vectors along the main faults (Jackson 1992), regional tectonic studies (Westaway 1990) and

GPS data (Reilinger et al. 1997; McClusky et al. 2000), which show the ETAP as being mainly subjected to a regime of strike-slip deformation.

The orientations of the left-lateral strike-slip faults vary from N20°E (Erzurum fault), to N50°E (Horasan Narman fault zone, Süphan fault) and N70°E (Kagizman fault), with a mean direction at N51°E (Fig. 6a). Right-lateral strike-slip fault azimuths are mainly N110°E (Tutak, Karayazi, Varto and Mus faults), N120°E (Caldiran fault), and N140°E (Balik Gölü and Hasantimur Gölü faults), with a mean N125°E direction (Fig. 6b). As previously proposed by Dewey et al. (1986), oblique-slip faults can be considered as the boundaries of upper crustal blocks (''flakes'') moving over a detachment surface located at the brittle–ductile boundary within the crust. This interpretation implies that only the upper crust of Anatolia is seismogenic, which is confirmed considering that the majority of earthquakes are restricted to the upper part of the crust (less than 20 km depth, Turkelli et al. 2003). Since the ETAP is a confined area, the crustal blocks do not have the possibility to move in a preferential direction and local compression may occur locally at their borders.

We did not observe many recent folds and thrusts in the ETAP, except along the southern margins of the Pasinler and Erzurum basins, along the northern shoulder of the Kars fault responsible for the Spitak earthquake (Philip et al. 1992), and at the fronts of the Bitlis and Caucasus belts. These observations are in agreement with seismotectonic data indicating that the deformation in the ETAP is accommodated by few minor thrust faults (Örgülü et al. 2003). Although thrust faults have a N090°E mean strike, there are discrepancies in the fault directions that vary from N45°E to N135°E (Fig. 6c), along which reverse motion may be associated with strike-slip movement. Compression occurs also at local scale at step-overs of strike-slip faults, forming push-up ridge structures mainly located along the Narman fault zone and Sengaya-Göle fault. One of the main conclusions in this paper is the absence of major compressional structures in the ETAP, showing that only a small part of the Arabia–Eurasia shortening is accommodated by crustal thickening.

Isolated volcanoes may be rooted on geometrical discontinuities associated with strike-slip faulting. They can be found in releasing-bend (Kandil volcano) and pull-apart (Süphan volcano) basins, and at horse-tail terminations (Nemrut volcano). Other edifices are elongate (Akbaba, Aragat, Ararat, Cavahet, Kel, Kisir, Legli, and Zor volcanoes; vents of the Kars volcanic plateau and south of the Tutak fault). In a similar way to that described in Iceland (Chorowicz et al. 1997) or in Central Anatolia (Dhont et al. 1998b), we assume that these volcanoes are related to open tension fractures serving as conducts for the magma. The mean trend of the elongate edifices is N005°E (Fig. 6e), consistent with a N95°E-directed extension.

We have plotted on a diagram (Fig. 7) the mean direction of these fault sets (Fig. 6a–c) and elongate volcanoes (Fig. 6e). Orientations of the structures fit fairly well with a regional tectonic regime characterized by N–S compression and E–W extension (Fig. 7). This strain pattern differs slightly from that of Koçyigit et al. (2001) who proposed NNW–SSE shortening and WSW–ENE extension.

In addition, we have identified some normal faults that mainly strike from N110°E to N130°E (Fig. 6d). The normal faults cross-cut all the previous volcanic and strike-slip tectonic structures: the Varto fault crosses the Bingöl volcano, the Hinis fault crosses the Karaçoban fault, and the Tuzluca fault crosses the Kagizman fault. Consequently, the normal faults, which are also of lesser importance and scarce in comparison to the strike-slip faults, were initiated later. The orientation of the normal faults is not consistent with a N–S compression and perpendicular extension; extensional deformation in the ETAP has to be explained by other mechanisms. An integrated geophysical survey across the ETAP presents data clearly demonstrating that the 2 km high topography of the ETAP is isostically undercompensated (Al-Lazki et al. 2003; Gök et al. 2000; Sanvol et al. 2003; Örgülü e al., 2003; Turkelli et al. 2003; Zor et al. 2003). Thus, the ETAP is not supported by thick crust but by hot mantle, and this leads to a model of active extension and lithospheric thinning. One of the explanations proposed for asthenospheric upwelling and lithospheric thinning is the break-off of the Arabian slab under Anatolia (Keskin 2003; Sengör et al. 2003). Another mechanism accounting for extensional deformation in Eastern Anatolia and the ETAP is the eastward propagation of the extension going on in the Aegean domain. Recent GPS data support the hypothesis that extension in the Aegean has effects far in the east beyond Karliova, and the westward motion of Anatolia would currently be driven completely by buoyancy forces (i.e., not by ''extrusion''), including foundering of the down-going African plate along the Hellenic trench (Reilinger et al. 2004). This result is in agreement with the interpretation of Chorowicz et al. (1999) who proposed that extensional deformation propagated through time from west to east along the NAF as far as at least the Varto fault. Moreover, Westaway and Arger (1996) also have shown that extension migrated eastward by progressive jumps of the eastern boundary of Anatolia, which is considered to be presently the EAF. The interpretations are that either the EAF initiated with the NAF at 5 Ma (Barka 1992; Westaway 1994; Platzman et al. 1998; Koçyigit and Beyhan 1998; Armijo et al. 1999), or independently between 3 and 1 Ma (Westaway and Arger 1996; Yürür and Chorowicz 1998; Barka et al. 2000). We propose here that the extensional deformation in Anatolia extended eastward beyond the EAF and reached the ETAP. Eastward migration of the extension is consistent with the volcanic activity that began slightly earlier in the western part of the plateau than in the eastern part (Keskin et al. 1998).

A striking feature is that compression, while being important in the Bitlis belt, is related to minor uplift

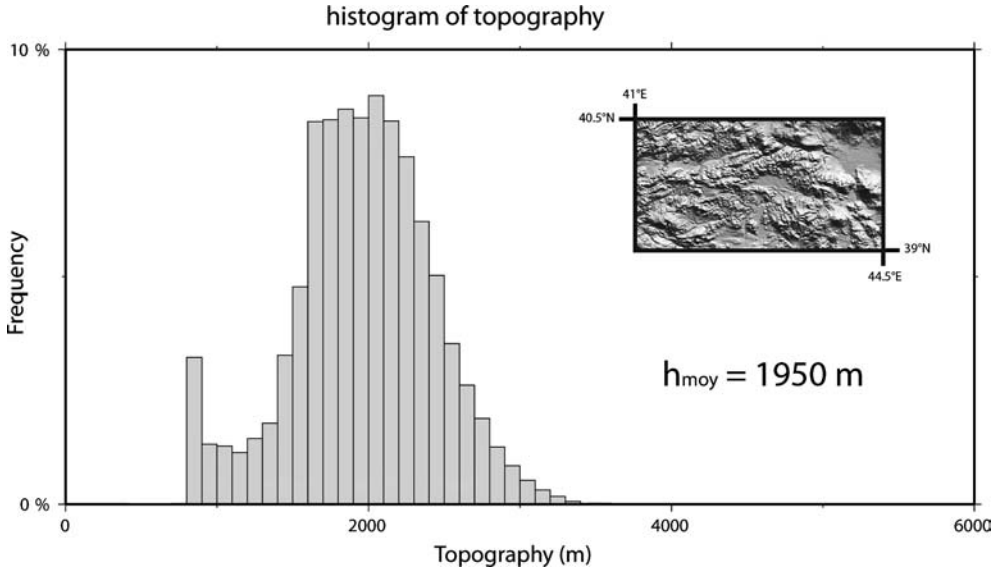

Fig. 5 Histogram of the topography of the Eastern Turkish–Armenian Plateau, computed in the central part of the plateau (frame). Mean elevation is 1,950 m. The peak value at ~800 m corresponds to the average altitude of the main basins (Erzurun, Pasinler, Agri and Ararat basins)

along this collisional zone. It forms a narrow (less than 50 km wide) tectonic edifice characterized by relatively low elevations, especially in its western part with peaks reaching no more than 2,000 m elevation. Our analysis shows that the Bitlis belt is bounded in the north by the half-ramp Mus basin, whose southern border is a north-dipping normal fault. Immediately east of the Mus basin, seismic profiles (Wong and Finckh 1978; Gülen 1984) display a series of NW–SE oblique-slip faults with major normal components bounding half-grabens tilted to the north. These features suggest that the Arabia–Eurasia continental collision is accompanied by extension north of the Bitlis belt.

Among the different views concerning the origin of the Bitlis massif, Yazgan (1984) and Yazgan and Chessex (1991) proposed that this metamorphic complex represents the northernmost extension of the Arabian plate. The massif consists of rocks metamorphosed from greenschist to upper amphibolite facies. This metamorphism is assumed to be related to the obduction of ophiolites over the Arabian platform in the late Campanian–early Maastrichtian (Yazgan and Chessex 1991). Metamorphic patterns locally involve blueschist facies south of the Pütürge massif, which corresponds to the western prolongation of the Bitlis complex. Hall (1974, 1980) recognized glaucophane-bearing schists in the frontal thrust belt. The morphology, structures and metamorphism of the Bitlis massif suggest that it can be considered as a metamorphic slice of crust, exhumed at the front of the Arabian continental subduction in a similar manner to that described by Chemenda et al. (1996) for Oman. The consequence of such a process is that the initial middle Miocene continental subduction was characterized by a low-compressional regime, and therefore compression in the ETAP was minor at this time.

Moreover, the uniform uplift of the plateau, the predominance of strike-slip faulting, the lack of major thrusts, and the occurrence of faults with normal-slip component do not support crustal thickening by compression from the middle Miocene onward. To the contrary, other clues favor a rather thin crust (45 km, Zor et al, 2003) and/or hot and thin lithospheric mantle in the ETAP: (1) high heat flow values (Kurtman and Baskan 1978; Mutlu and Güleç 1998); (2) a change in the nature of volcanism from calc-alkaline to alkaline (Innocenti et al. 1980, 1982; Yilmaz et al. 1987; Pearce et al. 1990); (3) a positive difference between observed gravity and isostatic gravity anomalies, showing that Turkey is isostasically under-compensated (Seber et al. 2001); (4) the occurrence of isolated volcanoes which are not related to faults (Akça, Akdogan, Bingöl, Ciplak, Hayal, Kavak, Meydan, and Tendurek volcanoes); and (5) inefficient Sn wave propagation (Gök et al. 2000, 2003; Sandvol et al. 2001) and very low Pn velocity zones (Al-Lazki et al. 2003) under the ETAP. In agreement with Gülen (1984), Pearce et al. (1990), Keskin et al. (1998, Keskin 2003), and Arger et al. (2000), we propose that uplift and lithospheric thinning of the ETAP are better explained from the partial replacement of lower continental lithosphere by upwelling hot upper mantle. As a consequence, the high elevations of the ETAP should not be related to the intracontinental convergence between the Arabian and Eurasian plates, but to mantle upwelling, leading to lithospheric thinning and recent extension.

This analysis has shown that the DEM constitutes first order valuable data for detailed geomorphic analysis at regional scale, helping to implement the mapping of the main neotectonic structures. Our main result is that the northward motion of Arabia is partitioned between (1) strike-slip faults, bounding blocks that move relatively to each others and elongate the crust perpendicularly to the direction of shortening, (2) minor folding and thrusting within the leading edge of the Arabian plate and along the Bitlis massif, and (3) compression,

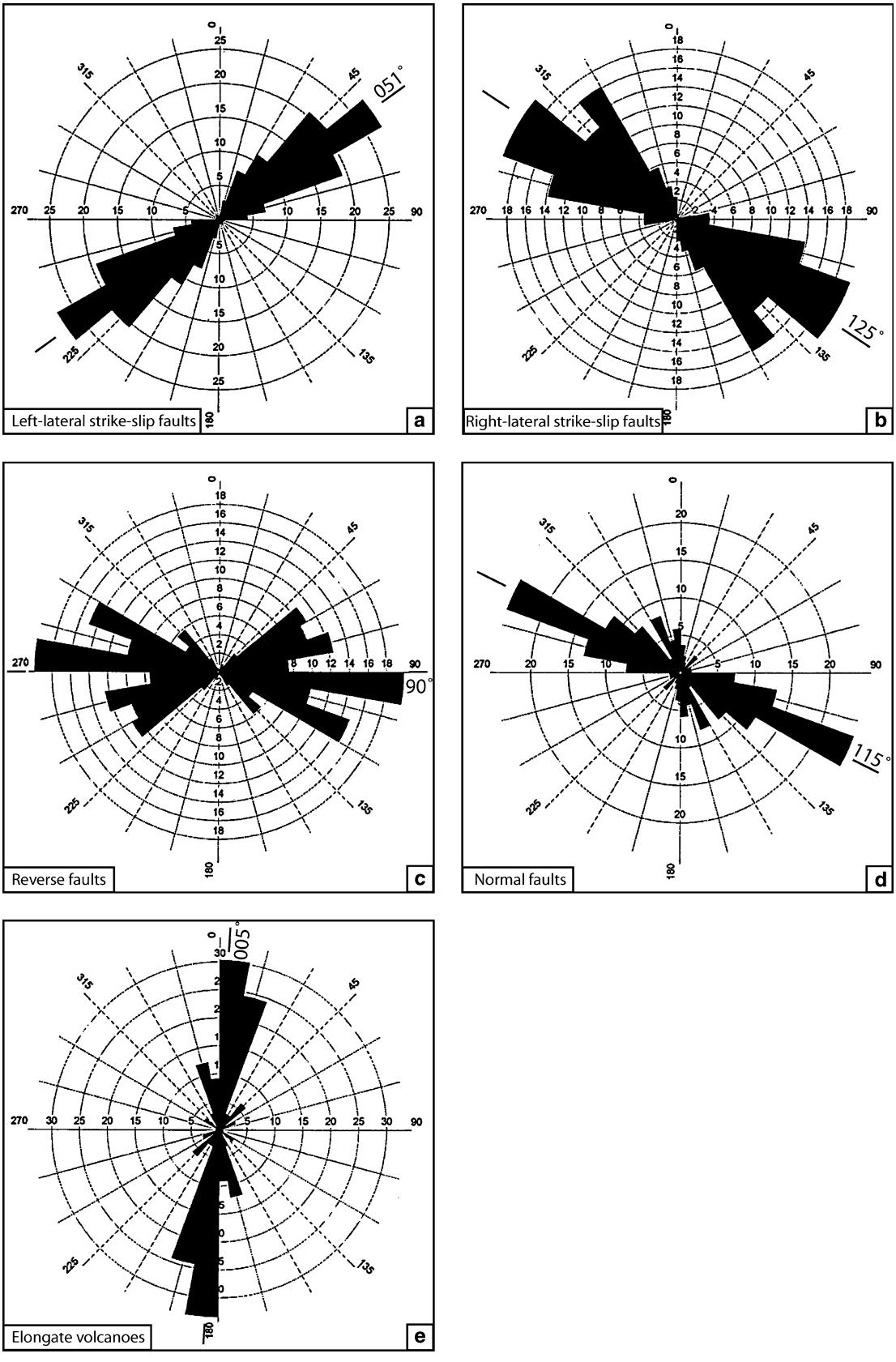

Fig. 6 Statistics showing the orientation and mean direction of structural features in the Eastern Turkish–Armenian Plateau. Rose diagrams are percentages of cumulative lengths. Directions of **a** left-lateral strike-slip faults, **b** right-lateral strike-slip faults, **c** reverse faults, **d** normal faults, and **e** elongate volcanoes have been measured on the DEM of Fig. 2

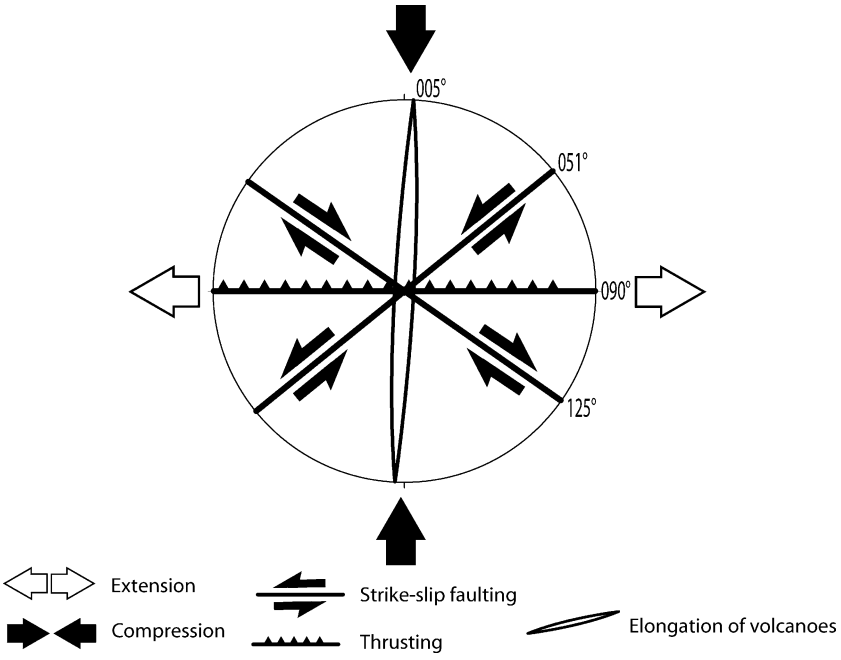

Fig. 7 Diagram showing the relationships between structural features of the Eastern Turkish–Armenian Plateau and the deformation. Mean value of each faults set (fig. 6a–c) and elongate volcanoes (Fig. 6d) are consistent with a N-S shortening and E-W lengthening tectonic regime

mainly located in the Caucassus. It is then difficult to consider that uplift of the ETAP is a consequence of the Arabia–Eurasia intracontinental collision. Our observations of strike-slip and superimposed extensional deformation in the plateau can be better interpreted in terms of lithospheric thinning related with westward escape of Anatolia whose motion is probably not due to the Arabia convergence but possibly to the Aegean slab retreat.

Acknowledgements This work has been funded by both the French CNRS (project PICS) and the Turkish TUBITAK (project YBAG-0078/DPT), with support from the French Embassy in Ankara and the Ministère des Affaires Etrangères in Paris. The authors are grateful to Onur Köse for his assistance in the realization of the DEM image. The paper benefited from constructive and thorough reviews of Clark Burchfiel and Rob Reilinger.

References

Adiyaman Ö, Chorowicz J, Köse O (1998) Relationships between volcanic patterns and neotectonics in Eastern Anatolia from analysis of satellite images and DEM. J Volcanol Geotherm Res 85:17–32

Al-Lazki A, Seber D, Sandvol E, Turkelli N, Mohamad R, Barazangi M (2003) Tomographic Pn velocity and anisotropy beneath the Anatolian plateau (eastern Turkey) and the surrounding regions. Geophys Res Lett 30(24):8043, DOI 10.1029/2003GL07391

Ambraseys N (2001) Reassessment of earthquakes, 1900–1999, in the Eastern Mediterranean and the Middle East. Geophys J Int 145:471–485

Ambraseys N, Zatopek A (1968) The Varto Ustukran earthquake of the 19 August 1966. Bull Seis Soc Am 58:47–102

Ambraseys NN, Jackson JA (1998) Faulting associated with historical and recent earthquakes in the Eastern Mediterranean region. Geophys J Int 133:390–406

Arger J, Mitchell J, Westaway RWC (2000) Neogene and quaternary volcanism of southeastern Turkey. In: Bozkurt E, Winchester JA, Piper JDA (eds) Tectonics and magmatism in Turkey and the surrounding area. Geol Soc Lond Spec Publ 173:459–487

Armijo R, Meyer B, Hubert A, Barka A (1999) Westward propagation of the North Anatolian fault into the northern Aegean: timing and kinematics. Geology 27:267–270

Arpat E, Saroglu F (1972) The East Anatolian Fault system: thoughts on its development. Bull Min Res Expl Inst Turkey 78:33–39

Arpat E, Saroglu F, Iz HB (1977) 1976 Caldiran Eathquake. Yeryuvari ve Insan 2:29–41

Atalay I (1978) Erzurum ovasi ve çevresinin jeomorfolojisi ve toprak cografyasi (Geomorphology and soil geography of the Mus plain and its surroundings) Ege Üniversitesi Edebiyat Fakültesi Yayinlari (Izmir) 24

Barka AA (1992) The North Anatolian Fault Zone. Annales Tectonicae 6:164–195

Barka AA, Kadinsky-Cade K (1988) Strike-slip fault geometry in Turkey and its influence on earthquakes activity. Tectonics 7:663–684

Barka A, Akkyüz HS, Cohen HA, Watchorn F (2000) Tectonic evolution of the Niksar and Tasova-Erbaa pull-apart basins, North Anatolian Fault Zone: their significance for the motion of the Anatolian block. Tectonophysics 322:243–264

Bommer JJ, Ambraseys NN (1989) The Spitak (Armenia, USSR) earthquake of 7 December 1988: a summary engineering seismology report Earthquake. Eng Struc 18:921–925

Bozkurt E (2001) Neotectonics of Turkey–a synthesis. Geodinamica Acta 14:3–30

Cello G, Crisci GM, Marabini S, Tortorici L (1985) Transtensive tectonics in the strait of Sicily: structural and volcanological evidence from the osland of Pantelleria. Tectonics 4;311–322

Chemenda AI, Mattauer M, Bokun AN (1996) Continental subduction and a mechanism for exhumation of high-pressure metamorphic rocks: new modeling and field data from Oman. Earth Planet Sci Lett 143:173–182

Chorowicz J, Bardintzeff J-M, Rasamimanana G, Chotin P, Thouin C, Rudant J-P (1997) An approach using SAR ERS images to relate extension fractures to volcanic vents: examples from Iceland and Madagascar. Tectonophysics 271:263–283

Chorowicz J, Dhont D, Gündogdu N (1999) Neotectonics in the eastern North Anatolian fault region (Turkey) advocates crustal extension: mapping from SAR ERS imagery and Digital Elevation Model. J Struct Geol 21:511–532

Chorowicz J, Emran A, Alem E M (2001) Tectonique et venues volcaniques en contexte de collision, exemple du massif néogène du Siroua (Atlas marocain) : effets combinés d'une transformante et de la suture panafricaine. Can J Earth Sci 38:411–425

Cisternas A, Philip H, Bousquet JC, Cara M, Deschamps A, Dortbath L, Dorbath C, Haessler H, Jimenez E, Nercessian A, Rivera L, Romanowicz B (1989) The Spitak (Armenia) earthquake of December 7, 1988: field observations, seismology and tectonics. Nature 339:675–679

Collet B, Parrot J-F, Taud H (2000) Orientation of absolute African plate motion revealed by tomomorphometric analysis of the Ethiopian dome. Geology 12:1147–1147

Dewey JF, Hempton MR, Kidd WSF, Saroglu F, Sengör AMC (1986) Shortening of continental lithosphere; the neotectonics of eastern Anatolia, a young collision zone. In: Coward MP, Ries AC (eds) Collision tectonics. Geol Soc Lond Spec Publ 19:3–36

Dhont D (1999) Etudes des déformations néogènes-quaternaires et de l'épaississement paléogène en Turquie Rapports avec l'échappement anatolien. PhD Thesis, Univ Paris 6, France

Dhont D, Chorowicz J, Köse O, Yürür T (1998a) Polyphased block tectonics along the North Anatolian Fault in the Tosya basin area (Turkey). Tectonophysics 299:213–227

Dhont D, Chorowicz J, Yürür T, Froger J-L, Köse O, Gündogdu N (1998b) Emplacement of volcanic vents and geodynamics of Central Anatolia, Turkey. J Volcanol Geotherm Res 85:33–55

Eyidogan H, Nalbant SS, Barka A, King G (1999) Static stress changes induced by the 1924 Pasinler (M = 68) and 1983 Horasan-Narman (M = 68) earthquakes, Northeastern Turkey. Terra Nova 11:38–44

Gök R, Türkelli N, Sandvol E, Seber D, Barazangi M (2000) Regional wave propagation in Turkey and surrounding regions. Geophys Res Lett 27:429–432

Gök R, Sandvol E, Türkelli N, Seber D, Barazangi M (2003) Sn attenuation in the Anatolian and Iranian plateau and surrounding regions. Geophys Res Lett 30(24):8042. DOI 10.1029/2003GL018020

Gülen L (1984) Sr, Nd, Pd isotope and trace elements geochemistry of calc-alkaline and alkaline volcanics, eastern Turkey. PhD Thesis, Massachussets Inst Tech

Hall R (1974) The structure and petrology of an ophiolitic melange near Mutki, Bitlis province, Turkey. PhD Thesis. University of London

Hall R (1980) Unmixing a mélange: the petrology and history of a disrupted and metamorphosed ophiolite, SE Turkey. Bull Geol Soc Am 87:1078–1088

Harrison JM, Lo CP (1996) PC-based 2D discrete Fourrier transform programs for terrain analysis. Computer Geosci 22:419–424

Innocenti F, Mazzuoli R, Pasquare G, Serri G, Villari L (1980) Geology of the volcanic area north of Lake Van (Turkey). Geol Rundsch 69:292–322

Innocenti F, Mazzuoli R, Pasquare G, Radicati D, Brozolo F, Villari L (1982). Tertiary and quaternary volcannism of the Erzurum-Kars area (Eastern Turkey): geochronological data and geodynamic evolution. J Volcanol Geotherm Res 13:223–240

Jackson J (1992) Partitioning of strike-slip and convergent motion between Eurasia and Arabia in eastern Turkey. J Geophys Res 97:12471–12479

Jackson J, McKenzie DP (1984) Active tectonics of the Alpine-Himalayan belt between western Turkey and Pakistan. Roy Astron Soc Geophys J 77:185–264

Jolivet L, Patriat M (1999) Ductile extension and the formation of the Aegean Sea. In: Durand B, Jolivet L, Horvath F, Séranne M (eds) The Mediterranean Basins: Tertiary Extension within the Alpine Orogen. Geol Soc Lond Spec Publ 156:427–456

Jolivet L, Daniel JM, Truffert C, Goffé B (1994) Exhumation of deep crustal metamorphic rocks and crustal extension in back-arc regions. Lithos 33:3–30

Keskin M, Pearce JA, Mitchell JG (1998) Volcano-stratigraphy and geochemistry of collision-related volcanism on the Erzurum-Kars Plateau, northeastern Turkey. J Volcanol Geotherm Res 85:355–404

Keskin M (2003) Magma generation by slab steepening and breakoff beneath a subduction-accretion complex: an alternative model for collision-related volcanism in Eastern Anatolia, Turkey. Geophys Res Lett 30(24):8046–8049

Kocyigit A (1985) Karayazi fault. Geol Soc Turkey Bull 28:67–72

Koçyigit A, Beyhan A (1998) A new intracontinental transcurrent structure: the Central Anatolian Fault Zone, Turkey. Tectonophysics 284:317–336

Koçyigit A, Yilmaz A, Adamia S, Kuloshvili S (2001) Neotectonics of East Anatolian Plateau (Turkey) and Lesser Caucasus: implication for transition from thrusting to strike-slip faulting. Geodinamica Acta 14:177–195

Korme T, Chorowicz J, Collet B, Bonavia FF (1997) Volcanic vents rooted on extension fractures and their geodynamic implications in the Ethiopian Rift. J Volcanol Geotherm Res 79:205–222

Kurtman F, Baskan E (1978) Mineral and thermal waters in the vicinity of Lake Van. In: Degens ET, Kurtman F (eds) The geology of the Lake Van. Miner Res Explor Inst (Ankara) 169:50–55

Kühni A, Pfiffner OA (2001) The relief of the Swiss Alps and adjacent areas and its relation to lithology and structure: topographic analysis from a 250 m DEM. Geomorphology 41:285–307

Mattauer M (1990) Arguments en faveur d'un diapir mantellique sous le plateau tibétain. C R Acad Sci Paris Sér II 310:1695–1770

McClusky S,S Balassanian S, A Barka A, C Demir C, S Ergintav S, I Georgiev I, O Gurkan O, M Hamburger M, K Hurst K, H Kahle H, Kastens K, Kekelidze G, King R, Kotzev V, Lenk O, Mahmoud S, Mishin A, Nadariya M, Ouzounis A, Paradissis D, Peter Y, Prilepin M, Reilinger R, Sanli I, Seeger H, Tealeb A, Toksoz MN, Veis G (2000) Global positioning system constraints on plate kinematics and dynamics in the eastern Mediterranean and Caucasus. J Geophys Res 105:5695–5719

McKenzie D (1972) Active tectonics of the Mediterranean regionGeophys. J R Astron Soc 30:109–185

Mutlu H, Guleç N (1998) Geochemical outline of thermal waters and geothermometry applications in Anatolia (Turkey). J Volcanol Geotherm Res 85:495–515

MTA (1989) Geological map of Turkey, scale 1:2,000,000, Ankara

Nakamura K (1977) Volcanoes as possible indicators of tectonic stress orientation-principle and proposal. J Volcanol Geotherm Res 2:1–16

Oguchi T, Aoki T, Matsuta N (2003) Identification of an active fault in the Japanese Alps from DEM-based hill shading. Comp Geosci 29:885–891

Opheim JA, Gudmundsson A (1989) Formation and geometry of fractures, and related volcanism of the Krafla fissure swarm, Northeast Iceland. Geol Soc Am Bull 101:1608–1622

Örgülü G, Aktar M, Türkelli N, Sandvol E, Barazangi M (2003) Contribution to the seismotectonics of Eastern Turkey from moderate and small size events. Geophys Res Lett 30(24): 8040. DOI 10.1029/2003GL018258

Pearce JA, Bender JF, De Long SE, Kidd WSF, Low PJ, Guner Y, Saroglu F, Yilmaz Y, Moorbath S, Mitchell JG (1990) Genesis of collision volcanism in Eastern Anatolia, Turkey. In: Le Fort P, Pearce JA, Pecher A (eds) Collision magmatism. J Volcanol Geotherm Res 44:189–229

Philip H, Rogozhin E, Cisternas A, Bousquet J-C, Borisov B, Karakhanian A (1992) The Armenian earthquake of 1988 December 7: faulting and folding, neotectonics and palaeoseismicity. Geophys J Int 110:141–158

Platzman ES, Tapirdamaz C, Sanver M (1998) Neogene anticlockwise rotation of central Anatolia (Turkey): preliminary palaeomagnetic and geochronological results. Tectonophysics 299:175–189

Rebaï S, Philip H, Dorbath L, Borissof B, Haessler H, Cisternas A (1993) Active tectonics in the Lesser Caucasus: coexistence of compressive and extensional structures. Tectonics 12:1089–1114

Reilinger RE, McClusky SC, Oral MB, King RW, Toksoz MN, Barka AA, Kinik I, Lenk O, Sanli I (1997) Global Positioning System measurements of present-day crustal movements in the Arabia-Africa-Eurasia plate collision zone. J Geophys Res 102:9983–9999

Reilinger RE, McClusky, S, Vernant, P (2004) GPS Constraints on continental deformation in the Eastern Mediterranean and Caucasus Region. Eos Trans., AGU, Fall Meeting Suppl., Abst., 85(47)

Sandvol E, Al-Damegh K, Calvert A, Seber D, Barazangi M, Mohamad R, Gök R, Tükelli N, Gürbüz C (2001) Tomographic imaging of Lg and Sn propagation in the Middle East Pure Appl Geophys 158:1121–1163

Sandvol E, Turkelli N, Zor E, Gok R, Bckler T, Gurbuz C, Seber D, Barazangi M (2003) Shear wave splitting in a young continent-continent collision. An example from Eastern Turkey. Geophys Res Lett 30(24):8041. DOI 1029/2003GL017390

Saroglu F, Güner Y (1979) Tutak fault, (in Turkish). Yeryuvari ve Insan 1:11–15

Saroglu F, Güner Y (1981) Dogu Anadolunun jeomorfolojik gelisimine etki eden ögeler, jeomorfoloji, tektonik, volkanizma iliskileri (in Turkish). Türkiye Jeol Kur Bült 24:267–282

Saroglu F, Emre Ö, Kuscu I (1992) Active fault map of Turkey general directorate of meneral and research exploration of Turkey Publication

Saroglu F, Yilmaz Y (1986) Dogu Anadolu'da neotektonik dönemdeki jeolojik evrim ve havza modelleri (in Turkish). Min Res Expl Inst Turkey Bull 110:143–164

Seber D, Sandvol E, Sandvol C, Brindisi C, Barazangi M (2001) Crustal model for the Middle East and North Africa region: implication for the isostatic compensation mechanism. Geophys J Int 147:630–638

Sengör AMC, Kidd WSF (1979) Post-collisional tectonics of the Turkish-Iranian plateau and a comparison with Tibet. Tectonophysics 55:361–376

Sengör AMC, Yilmaz Y (1981) Tethyan evolution of Turkey, a plate tectonic approach. Tectonophysics 75:181–241

Sengör AMC, Görür N, Saroglu F (1985) Strike-slip faulting and related basin formation in zones of tectonic escape : Turkey as a case study. In: Biddle KT, Christie-Blick N (eds) Strike-slip deformation, basin formation and sedimentation. Soc Econ Paloeontol Mineral Spec Publ 37: 227–264

Sengör AMC, Özderen S, Genç T, Zor E (2003) East Anatolian high plateau as a mantle-supported, north-south shortened domal structure. Geophys Res Lett 30(24):8045. DOI 10.1029/2003GL017858

Seymen I, Aydin A (1972) The Bingöl earthquake fault and its relation to the North Anatolian Fault Zone. MTA Bull 79:1–8

Silva PG, Goy JL, Zazo C, Bardaji T (2003) Fault-generated mountain fronts in southeast Spain: geomorphologic assessment of tectonic and seismic activity. Geomorphology 50:203–225

Tchalenko JS (1977) A reconnaissance of the seismicity and tectonics at the northern border of the Arabian plate (Lake Van region). Rev Géogr Phys Géol Dyn 19:189–208

Toksöz MN, Arpat E, Saroglu F (1977) East Anatolian earthquake of 24 November 1976. Nature 270:423–425

Turkelli N, Sandvol E, Zor E, Gok R, Bekler T, Al-Lazki A, Karabulut H, Kuleli S, Eken T, Gurbuz C, Bayraktutan S, Seber D, Barazangi M (2003) Seismogenic zones in Eastern Turkey. Geophys Res Lett 30(24):8039. DOI 10.1029/2003GL018023

Wallace RE (1968) Earthquake of the August 19, 1968, Varto area, Eastern Turkey. Bull Seismol Soc Am 58:11–45

Westaway R (1990) Seismicity and tectonic deformation in Soviet Armenia: implications for local earthquake hazard and evolution of adjacent regions. Tectonics 9:477–503

Westaway R (1994) Present-day kinematics of the middle east and the Eastern Mediterranean. J Geophys Res 99:12071–12090

Westaway R, Arger J (1996) The Gölbasi basin, Southern Turkey : a complex discontinuity in a major strike-slip fault zone. J Geol Soc London 153:729–744

Wong HK, Finckh P (1978) Shallow structures in Lake Van In: Degens ET, Kurtman F (Eds) The Geology of Lake Van Publ N° 169. Miner Res Explor Inst, Ankara, pp 6–10

Yazgan E (1984) Geodynamic evolution of the Eastern Taurus region In: Tekeli O, Göncüoglu, MC (Eds) Geology of the Taurus Belt MTA, Ankara, pp 199–208

Yazgan E, Chessex R (1991) Geology and tectonic evolution of the southeastern Taurides in the region of Malatya. TAPG Bull 3:1–42

Yilmaz Y, Saroglu F, Güner Y (1987) Initiation of the neomagmatism in East Anatolia. Tectonophysics 134:177–199

Yilmaz Y, Güner Y, Saroglu F (1998) Geology of the Quaternary volcanic centres of the East Anatolia. J Volcanol Geotherm Res 85:173–210

Yilmaz A, Adamia S, Chabukiani A, Chkhotua T, Erdogan K, Tuzcu S, Karabiyikoglu MF (2000) Structural correlation of the southern Transcaucasus (Georgia)-eastern Pontides (Turkey). In: Bozkurt E, Winchester JA, Piper JDA (eds) Tectonics and magmatism in Turkey and the surrounding areas. Geol Soc London Spec Publ 173:171–182

Yürür MT, Chorowicz J (1998) Recent volcanism, tectonics and plate kinematics near the junction of the African, Arabian, and Anatolian plates in the eastern Mediterranean. J Volcanol Geotherm Res 85:1–15

Zor E, Sandvol E, Gürbüz C, Türkelli N, Seber D, Barazangi M (2003) The crustal structure of the East Anatolian plateau (Turkey) from receiver functions. Geophys Res Lett 30(24):8044. DOI 10.1029/20003GL018192